Research Article

Journal of Biotechnology and its Applications

Gibbs Artifacts Removal with Nonlinearity

Gengsheng L. Zeng*

Department of Computer Science, Utah Valley University, Orem, Utah, USA;
Department of Radiology and Imaging Sciences, University of Utah, Salt Lake City, Utah, USA.

***Correspondence:**
Gengsheng L. Zeng, Department of Computer Science, Utah Valley University, Orem, Utah, USA; Department of Radiology and Imaging Sciences, University of Utah, Salt Lake City, Utah, USA.

Received: 11 Jul 2023; **Accepted:** 14 Aug 2023; **Published:** 20 Aug 2023

Citation: Gengsheng L. Zeng. Gibbs Artifacts Removal with Nonlinearity. J Biotechnology App. 2023; 2(1); 1-5.

ABSTRACT

Background: *Gibbs artifacts, appearing as oscillations or ringing around sharp edges or boundaries, are frequently encountered in image processing. They arise when the image's frequency components are adjusted, such as in image deblurring and sharpening. Linear methods are ineffective in reducing Gibbs artifacts; nonlinear methods may be more effective.*

Methods*: One such nonlinear method is the use of neural networks. This paper applies a simple convolutional neural network (CNN) to an image sharpening task and observes the effects of Gibbs artifacts. This network has only one convolutional layer, which consists of four channels. The well-known rectified linear unit (ReLU) is used as the nonlinear activation function.*

Results*: For simple one-dimensional (1D) and two-dimensional (2D), unrealistic case studies, the Gibbs artifacts are completely removed. The reason why the artifacts can be removed is explained.*

Conclusions: This simple case study illustrates the power of nonlinear functions and the use of multiple channels. In fact, this task can be achieved without using a neural network.

Keywords

Index Terms, Image processing, Artifacts, Neural Network.

Introduction

The Gibbs ringing artifact is a common artifact that appears as spurious oscillations near sharp edges in an image. These artifacts can degrade image quality and lead to errors in image interpretation. Gibbs artifacts appear when high frequency components are enhanced inconsistently. Linear methods are not as effective in reducing Gibbs artifacts, therefore *nonlinear* methods are commonly investigated. For example, in [1], a conceptually simple idea was proposed: first, the sharp boundaries were detected, and then the smooth region within the boundaries was processed. This approach avoided processing the edges. In a denoising task, lowpass filters are normally used. Avoiding the application of lowpass filters to the edges can preserve the image sharpness, while the noise is reduced in the relatively smooth regions.

In [2], a mask was generated for the overshooting regions. To detect and identify the overshooting regions is not easy. Once the overshoot region was identified, an overshoot ripple filter was used to smooth out the overshoot ripples. Simple nonlinear filters such as the median filter, applied in the image domain or in the wavelet domain, were found effective for reducing Gibbs artifacts [3]. The median filter is a special case of the rank-order filters, its main application is to remove the salt-and-pepper noise.

It had been observed that the amplitude of the Gibbs ringing is directly proportional to the height of the image discontinuity. If the height of the discontinuity could be reduced, the subsequent ringing would also be reduced. To achieve this, separating the

image into stratified layers or partitions reduced the height of the discontinuity significantly. Each partition was then filtered separately and recombined nonlinearly to yield the final filtered image [4]. This method weakens the filtering of image edges that have large discontinuities, reducing the Gibbs phenomenon while simultaneously reducing the image noise.

Another nonlinear method to reduce Gibbs artifacts while deblurring an image was to temporarily remove the background [5]. If the target features (e.g., hot lesions) had a positive background, removing the background before applying the post-processing filter significantly helped with target deblurring and suppressing Gibbs artifacts. This method works only if a nonnegativity constraint is used, such as the iterative maximum-likelihood expectation-maximization (ML-EM) algorithms and the similar multiplicative updating algorithms [6].

Bayesian methods are considered nonlinear and effective. For example, the total variation (TV) norm of the image can be used to promote the piecewise constant appearance in the image [7,8]. Most Bayesian methods are iterative in nature. However, the downside of the TV norm minimization is that some important image details are removed or suppressed unintentionally. Of course, machine learning methods [9] are the state-of-the-art approaches in all aspects of medical imaging, including image reconstruction, denoising, deblurring, and artifact reduction. In this paper, we use a simple case study to explain how a neural network can reduce Gibbs artifacts.

Methods

Our simple hypothetical study cases in this paper are for illustrative purposes only and are not intended for real-world applications. The task is image deblurring, and we assume that we have a large dataset of data/label pairs to train a convolutional neural network (CNN). The labels represent the unblurred true image, which contains piecewise-constant regions. The input data consists of the corresponding blurred images.

To remove the Gibbs ringing artifacts while deblurring the image, we use a single layer of CNN. The output of a convolutional neuron is calculated using an inner product and a bias:

$$Out_c(x,y) = \sigma(In(x,y) ** h_c(x,y) + Bias_c(x,y)), \quad (1)$$

where *In (x,y)* is the input image, Out_c *(x,y)* is the c^{th} channel's output, h_c *(x,y)* is the convolution kernel of the c^{th} channel, $Bias_c$ *(x,y)* is the bias of the c^{th} channel, and σ is the ReLU (rectified linear unit) activation function defined as

$$\sigma(t) = max(0,t). \quad (2)$$

There are *M* channels in this CNN layer. The neural network's final output is a weighted sum of the channel outputs as

$$Final(x,y) = \sum_{c=1}^{M} w_c \times Out_c(x,y), \quad (3)$$

where w_c is the weighting coefficient for the c^{th} channel.

If the ReLU function is disabled and all biases are set to zero in (1), then each channel in (1) produces a linearly filtered image. If a convolution kernel is not a low-pass filter kernel, it is most likely that the channel output image will have Gibbs ringing artifacts. We argue that the combination of biases, the ReLU function, and multiple channels together can remove the Gibbs artifacts in our special case. The principle is explained in Figure 1 using a one-dimensional (1D) example.

The true function *f(t)* is given in Figure 1(a), and its ripple-corrupted version *g(t)* is shown in orange in Figure 1(b). There are four channels, and four bias values, b_1, b_2, b_3, b_4, are shown. Figure 1(c) shows the result of

$$\sigma(g(t) - b_1) - \sigma(g(t) - b_2), \quad (4)$$

and Figure 1(d) shows the result of

$$\sigma(g(t) - b_3) - \sigma(g(t) - b_4). \quad (5)$$

Finally, Figure 1(e) shows the final processed result, which is a weighted sum of (4) and (5) as

$$\frac{A}{b_2 - b_1}\sigma(g(t) - b_1) - \frac{A}{b_2 - b_1}\sigma(g(t) - b_2)$$
$$\frac{A}{b_2 - b_1}\sigma(g(t) - b_1) - \frac{A}{b_2 - b_1}\sigma(g(t) - b_2) \quad (6)$$

Expression (6) shows the final output, which is the weighted sum of the four channels. The selection of the biases, b_1, b_2, b_3, b_4, are not unique. The neural network thus has many optimal solutions.

The most important 'trick' of removing the ringing artifacts is the 'difference' operation shown in Figures 1(c) and (d). In expression (4), we observe that in the interval (1, 3), both $g(t)-b_1$ and $g(t)-b_2$ are positive; the ReLU function σ can be ignored. Thus, we have

$$\sigma(g(t) - b_1) - \sigma(g(t) - b_2) = (g(t) - b_1) - (g(t) - b_2) = b_2 - b_1, \quad (7)$$

which is a constant in the interval (1, 3). The ripples in *g(t)* are completely removed as shown in Figure 1(c).

Similarly, in expression (5), we observe that in the interval (1, 5), both $g(t)-b_3$ and $g(t)-b_4$ are positive; the ReLU function σ can be ignored. Thus, we have

$$\sigma(g(t) - b_3) - \sigma(g(t) - b_4) = (g(t) - b_3) - (g(t) - b_4) = b_4 - b_3, \quad (8)$$

which is a constant over (1, 5). The ripples in $g(t)$ and the large jump at $t = 3$ are completely removed as shown in Figure 1(d).

We see two boxcars, one in Figure 1 (c) and the other in Figure 1(d). The weighted sum of these two boxcars approximates the original function as illustrated in Figure 1(e). The weighting factors are shown in (6). We must point out that the weighting factors in (6) are determined by parameters *A* and *B*. Therefore,

this method works only if the function *f(t)* is a piecewise-constant function and only takes the values *A* and *B*.

Using the jargons of machine learning, the 'labels' are piecewise-constant functions and only take the values *A* and *B*. After training, the network does not remember any of the training function pairs. Instead, the network learns the values *A* and *B*, and then selects the bias values, b_1, b_2, b_3, b_4, which are not unique. In other words, the loss function of the network has infinite numbers of optima and may converge to any of them.

Results and Discussion

After explanation of the working principle in Section II, Section III presents two study cases. In these two studies, the true 1D or 2D functions were piecewise-constant and only took the five values: 0, 0.25, 0.5, 0.75 and 1. The functions were randomly generated.

For the one-dimensional (1D) case, the true function is displayed in Figure 2(a), where the function $f_{original}$ is defined on 0, 1, 2, …, 256. Then the function was blurred with a Gaussian point spread function of variance 9.5, resulting in $f_{blurred}$ shown in Figure 2(b). In the next step, the iterative Richardson-Lucy algorithm [10,11] was used to deblur the function $f_{blurred}$ with the same Gaussian point spread function. The number of iterations was 50, and the resultant function f_{RL} is shown in Figure 2(c), where some severe Gibbs ringing artifacts are clearly observable.

After 8 channels were used and proper bias values were selected, the ripples were successfully removed, and the final result f_{final} is shown in Figure 2(d). As a matter of fact, our over-simplified Gibbs artifact removal task is fairly trivial, because the true function values are discrete and known (or can be learned). There are many other ways to achieve the same results without using the ReLU function. Here is an alternative approach. We set up four threshold values as: t_1=0.125, t_2=0.375, t_3=0.625, and t_4=0.875. To remove the ringing ripples, we simply use the following expression (9).

$$f_{final}(t) = \begin{cases} 0 & if \quad f_{RL}(t) < t_1 \\ 0.25 & if \quad t_1 \le f_{RL}(t) < t_2 \\ 0.5 & if \quad t_2 \le f_{RL}(t) < t_3 \\ 0.75 & if \quad t_3 \le f_{RL}(t) < t_4 \\ 1 & if \quad t_4 \le f_{RL}(t) < t_5. \end{cases} \tag{9}$$

In the same way, for a two-dimensional (2D) example, Figure 3 shows how a one-layer CNN unblurs an image without producing Gibbs artifacts. In both 1D and 2D cases, the Gibbs ringing artifacts were successfully removed. The 'trick' is to use multiple channels, a nonlinear activation function, and some carefully selected bias values. An alternative way to do it is to use the expression (9).

Conclusions

This paper suggests that nonlinear methods are more powerful and can achieve better results than linear methods. The Gibbs ringing artifact removal problem has been troubling the image processing communities for many years. It seems that linear methods such as lowpass filtering are less effective to battle the Gibbs artifacts. Nonlinear methods have the flexibility to explore more ways to battle the Gibbs artifacts.

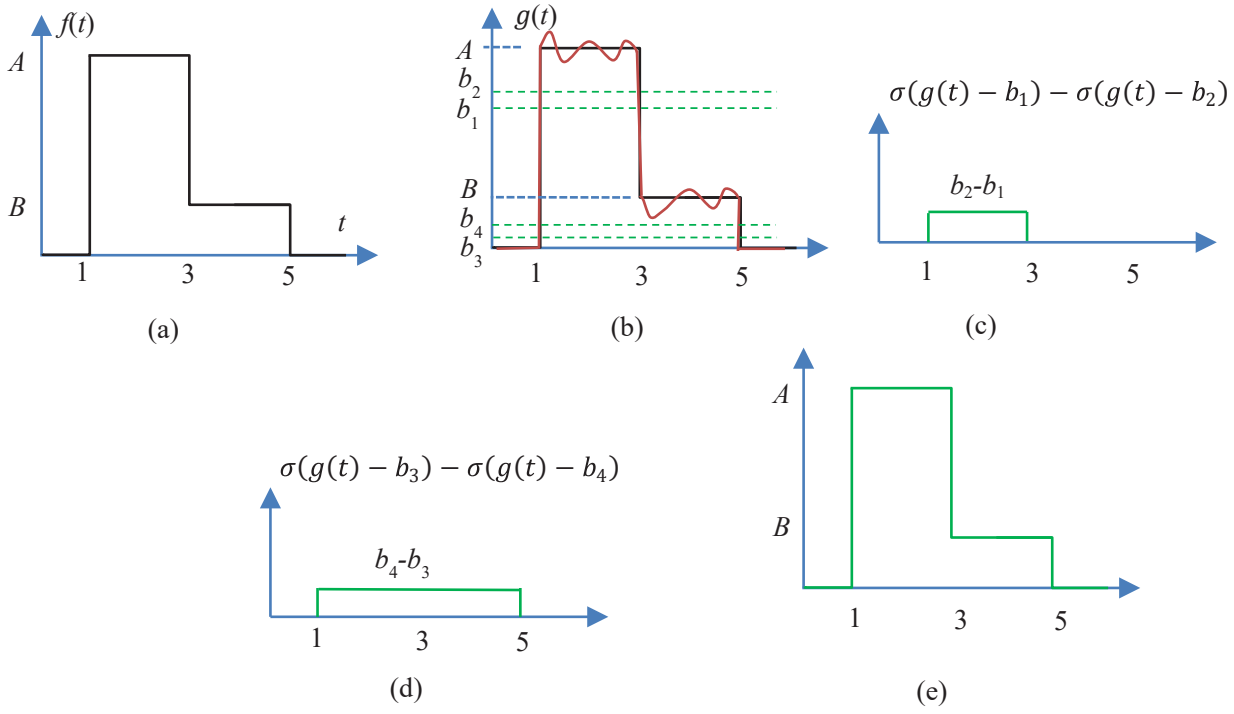

Figure 1: Steps to show how a CNN removes the Gibbs artifacts. (a) The original true function. (b) A function with ripple artifacts shown in orange color. (c, d) The combination of the biases, the ReLU function, and multiple channels can produce 'boxcar' functions. (e) Weighted sum of (c) and (d).

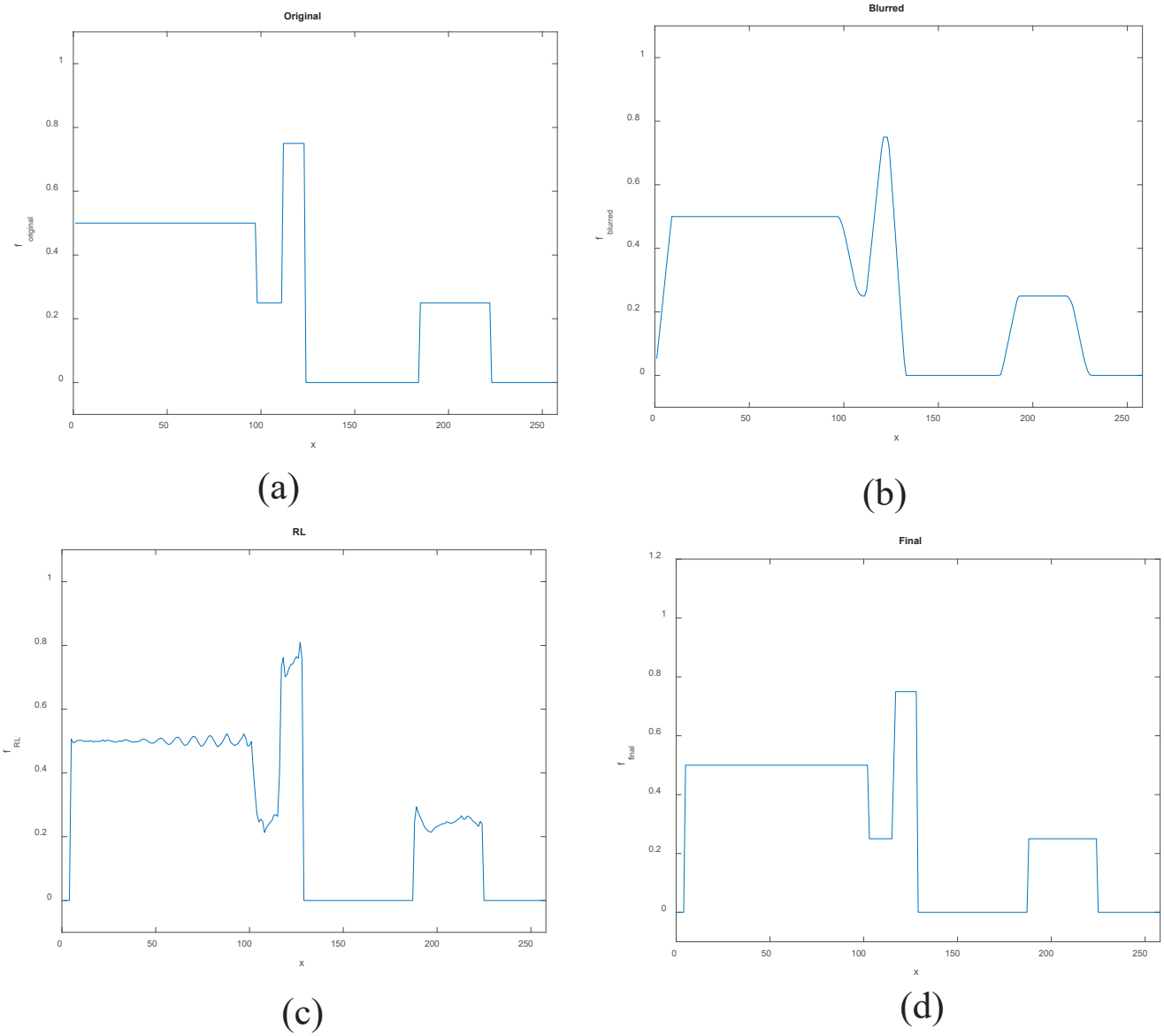

Figure 2: A one-dimensional example. (a) The original true function. (b) Blurred function by a Gaussian kernel. (c) Deblurred function by the iterative Richardson-Lucy algorithm. (d) Processed function generated by the summation of perceptron outputs.

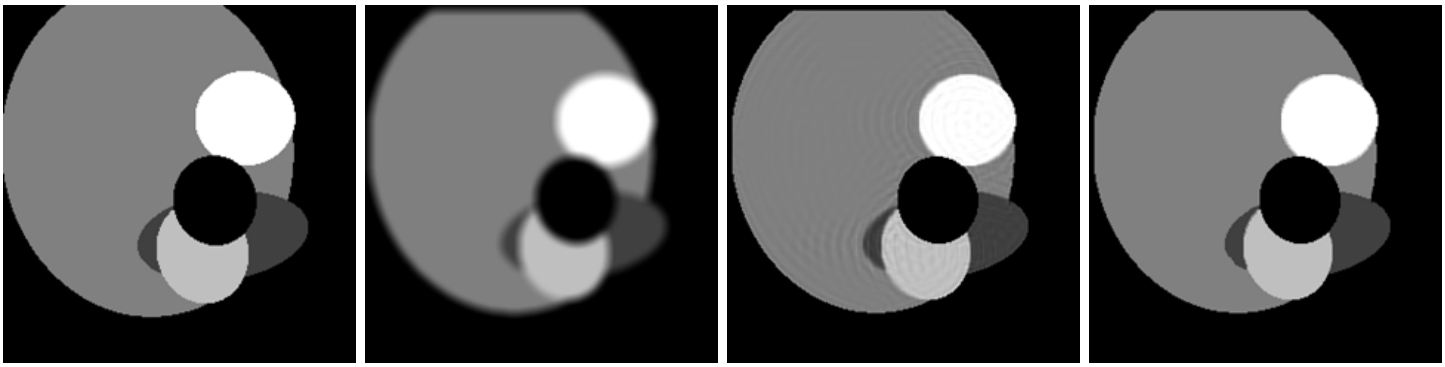

(a) (b) (c) (d)

Figure 3: A two-dimensional example. (a) The original true image. (b) Blurred image by a Gaussian kernel. (c) Deblurred function by the iterative Richardson-Lucy algorithm. (d) Processed image generated by the summation of perceptron outputs.

The machine learning models are nonlinear, because they use nonlinear activation functions such as the ReLU function. One distinguishing advantage of using a machine learning method is that the network can automatically extract some useful features from the training data. The useful features in the data presented in this paper are the fixed discrete image values. Once the features are discovered, to find a solution becomes easier.

This paper uses a simple image deblurring situation to explain that a multi-channel, one-layer CNN is able to produce deblurred images that are free of Gibbs artifacts. The convolution actions beblur the image and produce Gibbs artifacts as the side effects. The bias and ReLU activation remove the artifacts. Even though our task is over-simplified, the practical applications with discrete image values may exist in the real world. For this over-simplified task, we do not have a linear solution to remove the Gibbs artifacts.

As suggested by expression (9), the CNN model is not the only approach to provide a nonlinear solution. Some alternative nonlinear solutions exist. In general, the Gibbs artifact removal problem is still open. More investigations and new results are yet to come.

References

1. Archibald R, Gelb A. A method to reduce the Gibbs ringing artifact in MRI scans while keeping tissue boundary integrity. IEEE Trans Med Imaging. 2002; 21: 305-319.
2. Lim H, Park H. A ringing-artifact reduction method for block-DCT-based image resizing. IEEE Transactions on Circuits and Systems for Video Technology. 2011; 21: 879-889.
3. Shin GS, Kang MG. Ringing artifact reduction in the wavelet-based denoising. 2004 IEEE International Conference on Acoustics, Speech, and Signal Processing, Montreal, QC, Canada. 2004; 3: iii-233.
4. Zeng GL, Allred RJ. Partitioned image filtering for the reduction of the Gibbs phenomenon. J Nucl Med Tech. 2009; 37: 96-100.
5. Zeng GL. Gibbs artifact reduction by non-negativity constraint. J Nuc Med Tech. 2011; 39: 213-219.
6. Zeng GL. Emission expectation-maximization look-alike algorithms for x-ray CT and other applications. Medical Physics. 2018; 45: 3721-3727.
7. Sarra SA. Digital total variation filtering as postprocessing for chebyshev pseudospectral methods for conservation laws. Numerical Algorithms. 2006; 41: 17-33.
8. Panin VY, Zeng GL, Gullberg GT. Total variation regulated EM algorithm. IEEE Trans. Nucl Sci. 1999; 46: 2202-2210.
9. Rai S, Bhatt JS, Patra SK. Augmented noise learning framework for enhancing medical image denoising. IEEE Access. 2021; 9: 117153-117168.
10. Richardson WH. Bayesian-based iterative method of image restoration. Journal of the Optical Society of America. 1972; 62: 55-59.
11. Lucy LB. An iterative technique for the rectification of observed distributions. Astronomical Journal. 1974; 79: 745-754.